

Space-time sensors using multiple-wave atom levitation

F. Impens^{1,2} and Ch. J. Bordé^{1,3}

¹*SYRTE, Observatoire de Paris, 61 Avenue de l'Observatoire, 75014 Paris, France*

²*Instituto de Física, Universidade Federal do Rio de Janeiro, Caixa Postal 68528, 21941-972 Rio de Janeiro, RJ, Brazil*

³*Laboratoire de Physique des Lasers, Institut Galilée, F-93430 Villetaneuse, France*

(Received 4 September 2008; published 21 September 2009)

The best clocks to date control the atomic motion by trapping the sample in an optical lattice and then interrogate the atomic transition by shining on these atoms a distinct laser of controlled frequency. In order to perform both tasks simultaneously and with the same laser field, we propose to use instead the levitation of a Bose-Einstein condensate through multiple-wave atomic interferences. The levitating condensate experiences a coherent localization in momentum and a controlled diffusion in altitude. The sample levitation is bound to resonance conditions used either for frequency or for acceleration measurements. The chosen vertical geometry solves the limitations imposed by the sample free fall in previous optical clocks using also atomic interferences. This configuration yields multiple-wave interferences enabling levitation and enhancing the measurement sensitivity. This setup, analogous to an atomic resonator in momentum space, constitutes an attractive alternative to existing atomic clocks and gravimeters.

DOI: [10.1103/PhysRevA.80.031602](https://doi.org/10.1103/PhysRevA.80.031602)

PACS number(s): 03.75.Dg, 06.30.Ft, 06.30.Gv, 37.25.+k

The light-matter interaction enables the exchange of momentum between an electromagnetic field and atoms: each atom emitting or absorbing a photon experiences simultaneously a change in internal level and a recoil reflecting momentum conservation. This well-controlled momentum transfer can be used to engineer correlations between the motional and the internal atomic states. This is the principle underlying Bordé-Ramsey atom interferometers [1–3], which are the building blocks of our system. Such interferometers consist in the illumination of moving two-level atoms with a first pair of light pulses separated temporally and propagating in the same direction (Fig. 1), followed by a second pair of pulses coming from the opposite direction. Each pulse operates a $\pi/2$ rotation on the vector representing the atomic density matrix on the Bloch sphere: applied on a given internal state, it acts as an atomic beam splitter by creating a quantum superposition of two atomic states with distinct internal levels and momenta. Horizontal Bordé-Ramsey interferometers have been used to build optical clocks [4]. This system presents, however, two drawbacks: the free fall of the atoms through the transverse lasers probing their transition limits the interrogation time and induces undesirable frequency shifts [5]. This led the metrology community to privilege atomic clocks [6] built around atomic traps [7], able to control the sample position. Such systems have become sufficiently accurate to probe fundamental constants [8]. We propose instead to circumvent these limitations with a multiple-wave atom interferometer [9] in levitation, which comprises a succession of vertical Bordé-Ramsey atom interferometers. This strategy combines the best aspects of optical clocks based on atom traps and on atom interferometers: it prevents the sample free fall without using optical potentials likely to cause spurious frequency shifts. The recent experimental achievement [10] of a sustainable levitation of coherent atomic waves with synchronized light pulses [11] strongly supports the feasibility of this method.

Our purpose is to provide a controlled vertical momentum transfer to the atoms, eventually enabling their levitation, through the repetition of a four-vertical $\pi/2$ -pulse sequence. Momentum kicks are achieved by performing two successive

population transfers with vertical pulses propagating in opposite directions: starting from the adequate atomic state, one obtains successively the absorption of an upward photon followed by the emission of a downward one, imparting a net upward momentum to the atoms. This leads us to consider the point illustrated in Fig. 1: when do two time-separated $\pi/2$ pulses realize a full population transfer?

To achieve this, one must indeed compensate the phase induced by the external atomic motion in the time interval through fine-tuned laser phases. This phase adjustment is at the heart of our proposal since it provides the resonance condition serving for the laser frequency stabilization in the clock operation. The $\pi/2$ -pulse sequence then yields a *conditional* momentum transfer, controlled by this resonance condition, which distinguishes this process from atomic Bloch oscillations [12]. Long π pulses, realizing conditional population transfers [3], could also perform such levitation [11,10]. Yet there are several benefits in privileging $\pi/2$ pulses: the atomic illumination time is drastically reduced, the pulses address a broader distribution of atomic momenta, and a better sensitivity is obtained through a wider interferometric area [3]. To obtain the resonance condition, we consider a dilute sample of two-level atoms evolving in the

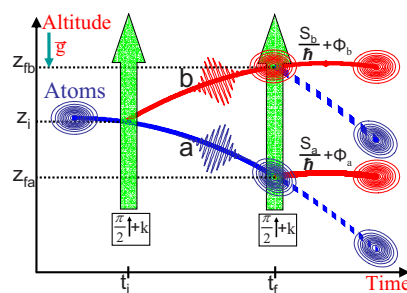


FIG. 1. (Color online) Action of a pair of copropagating $\pi/2$ pulses on a free-falling atomic wave packet. The phase difference between the two outgoing wave packets comes from the classical action and laser phase acquired on each path and from the distance of their centers.

gravity field-taken as uniform—according to the Hamiltonian $H=p^2/2m+mgz$. It is initially in the lower state a and described by the Gaussian wave function [13]

$$\psi_a(\mathbf{r}, t_0) = \frac{\pi^{-3/2}}{\sqrt{w_{x0}w_{y0}w_{z0}}} \exp \left[-\frac{1}{2} \left(\frac{(x-x_i)^2}{w_{x0}^2} + \frac{(y-y_i)^2}{w_{y0}^2} + \frac{(z-z_i)^2}{w_{z0}^2} \right) + \frac{i}{\hbar} \mathbf{p}_{ia}(t_0) \cdot (\mathbf{r}-\mathbf{r}_i) \right].$$

After two $\pi/2$ pulses, performed at the times t_i and $t_f=t_i+T$, the initial wave packet has been split into four packets following two possible intermediate trajectories. The excited state wave function receives two wave-packet contributions coming from either path and associated with the absorption of a photon at times t_i and t_f , of common central momentum $\mathbf{p}_f=\mathbf{p}_i+\hbar\mathbf{k}+m\mathbf{g}T$ and respective central positions \mathbf{r}_{fa} and \mathbf{r}_{fb} . These wave packets acquire a phase $S_{a,b}/\hbar$ reflecting the action on each path [16] and a laser phase $\phi_{a,b}$ evaluated at their center for the corresponding interaction time. Both contributions to the excited state are phase matched if the following relation [14] is verified:

$$-\mathbf{p}_f \cdot \mathbf{r}_{fa} + S_a + \hbar\phi_a = -\mathbf{p}_f \cdot \mathbf{r}_{fb} + S_b + \hbar\phi_b. \quad (1)$$

The terms $\mathbf{p}_f \cdot \mathbf{r}_{fa,b}$ reflect the atom-optical path difference between both wave packets at their respective centers. The central time $t_c=(t_i+t_f)/2$ is used as the phase reference for the two successive pulses. The phases ϕ_b and ϕ_a provided, respectively, by the first and the second $\pi/2$ pulses read $\phi_{b,a}=\mathbf{k} \cdot \mathbf{r}_{i,fa} - \omega_{1,2}(t_{i,f}-t_c) + \phi_{1,2}^0$. The action is given by $S_{a,b}=m\mathbf{g}^2T^3/3 + \mathbf{p}_{ia,ib} \cdot \mathbf{g}T^2 + (p_{ia,ib}^2/2m - mgz_i - E_{a,b})T$. Condition (1) is fulfilled if the frequencies $\omega_{1,2}$ of the first and the second pulses are set to their resonant values

$$\omega_{1,2} = \frac{1}{\hbar} \left(E_b + \frac{(\mathbf{p}_{1,2} + \hbar\mathbf{k})^2}{2m} - E_a - \frac{p_{1,2}^2}{2m} \right) \quad (2)$$

with $\mathbf{p}_1=\mathbf{p}_i$ and $\mathbf{p}_2=\mathbf{p}_i+m\mathbf{g}T$ and if the constant phases $\phi_{1,2}^0$ satisfy $\phi_1^0=\phi_2^0$. If these conditions are fulfilled, and if the sample coherence length w is much larger than the final wave-packet separation $|\mathbf{r}_{fa}-\mathbf{r}_{fb}|$, or equivalently if the Doppler width $k\Delta p/m$ experienced by the traveling atoms is much smaller than the frequency $1/T$, one obtains an almost fully constructive interference in the excited state. The succession of two $\pi/2$ pulses then mimics very efficiently a single π pulse, with the quantum channel to the lower state being shut off by destructive interferences. A key point is that condition (1), expressing the equality of the quantity $I=-\mathbf{p}_f \cdot \mathbf{r}_f + S + \hbar\phi$ for both paths, is independent of the initial wave-packet position. This property allows one to address simultaneously the numerous wave packets generated in the $\pi/2$ pulse sequence. Applying a second sequence of two $\pi/2$ pulses with downward wave vectors [15], one obtains a vertical Bordé-Ramsey interferometer bent by the gravity field sketched on Fig. 2.

Starting with a sufficiently coherent sample in the lower state, and with well-adjusted frequencies (2) and ramp slopes, the previous discussion shows that a net momentum transfer of $2\hbar\mathbf{k}$ is provided to each atom during the interferometric sequence. For the special interpulse duration

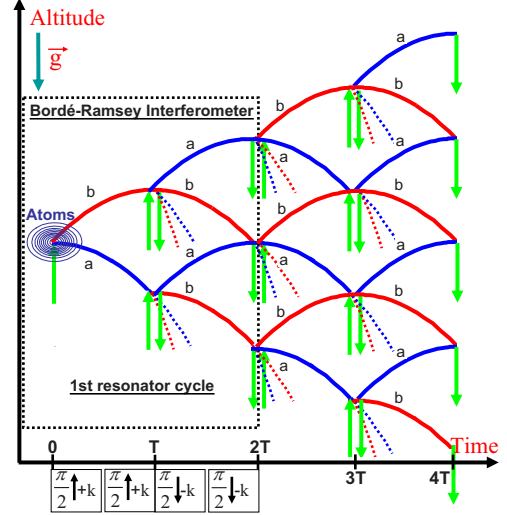


FIG. 2. (Color online) Levitating atomic trajectories in the sequence of pulses. The first four pulses generate a vertical Bordé-Ramsey interferometer. The central positions of the wave packets explore a network of paths which doubles at each laser pulse.

$$T := T^0 = \frac{\hbar k}{mg}, \quad (3)$$

these atoms end up in the lower state with their initial momentum. Two major benefits are then expected. First, the periodicity of the sample motion in momentum gives rise to levitation. Second, only two frequencies, given by Eq. (2), are involved in the successive resonant pairs of $\pi/2$ pulses. In particular, the first and the fourth pulses of the Bordé-Ramsey interferometer, as well as the second and the third one, correspond to identical resonant frequencies: $\omega_1^0=\omega_4^0$ and $\omega_2^0=\omega_3^0$.

If the previous conditions are fulfilled, the repetition of the interferometer sequence gives rise to a network of levitating paths—sketched on Fig. 2—reflecting the diffusion of the atomic wave in the successive light pulses. The same laser field is used to levitate the sample and to perform its interrogation, generating a clock signal based on either one of the two frequencies ω_1^0, ω_2^0 . Our measurement indeed rests on the double condition (2) and (3), which must be fulfilled to ensure this periodic motion: should the parameters $(T, \omega_{1,2,3,4})$ differ from their resonant values $(T^0, \omega_{1,2,3,4}^0)$, the outgoing channels would open again and induce losses in the levitating cloud, which can be tracked by a population measurement. We expect multiple-wave interference to induce a narrowing of the resonance curve associated with the levitating population around this condition.

We have investigated this conjecture through a numerical simulation. The considered free-falling sample is taken at zero temperature, sufficiently diluted to render interaction effects negligible, and described initially by a macroscopic Gaussian wave function. Its propagation in between the pulses is obtained by evaluating a few parameters: central position and momentum following classical dynamics, widths satisfying $w_{x,y,z}^2(t) = w_{x,y,z}^2(t_0) + [\hbar^2/(4m^2w_{x,y,z}^2)](t-t_0)^2$, and a global phase proportional to the action on the classical

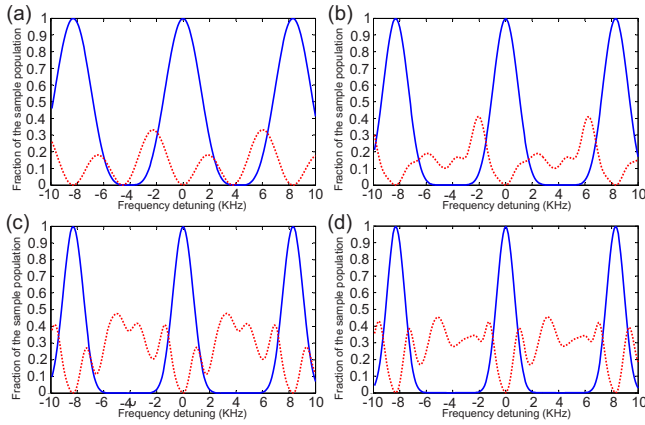


FIG. 3. (Color online) Fraction of the total sample population levitating (full line) and falling (dashed line) in state a after one, two, three, and four sequences of four pulses as a function of the frequency detuning $\delta\omega$ (kHz) ($\omega_{1,2,3,4} := \omega_{1,2,3,4}^0 + \delta\omega$) and for a resonant interferometer duration $2T^0 \approx 1.5$ ms.

path [16]. Interaction effects may be accounted for perturbatively with generalized $ABCD$ matrix propagation formalism [18]. The diffusion of atomic packets on the short light pulses is efficiently modeled by a position-dependent Rabi matrix [3] evaluated at the packet center. While the evolution of each wave packet is very simple, their number—doubling at each light pulse—makes their bookkeeping a computational challenge. This difficulty, intrinsic to the classical simulation of an entangled quantum state, has limited our investigation to a sequence of 16 pulses, involving 28 levitating Bordé-Ramsey interferometers associated with the resonant paths. The number of atomic waves involved ($N \approx 64000$) is nonetheless sufficient to probe multiple-wave interference effects.

The atomic transition used in this setup should have level lifetimes longer than the typical interferometer duration (ms). Possible candidates are the Ca, the Sr, the Yb, and the Hg atoms, which have narrow clock transitions in their internal structures. These atoms should be cooled at a temperature in the nanokelvin range, preferably in a vertical cigar-shaped condensate, in order to guarantee a sufficient overlap of the interfering wave packets and preserve a significant levitating atomic population. We consider a cloud of coherence length $w = 100 \mu\text{m}$ much larger than the wave packets separation $2h \approx 15 \mu\text{m}$. Figure 3 shows the levitating and the falling atomic population in the lower state as a function of the frequency shift $\delta\omega$ from the resonant frequencies $\omega_{1,2,3,4}^0$. It reveals a fully constructive interference in the levitating arches when resonance conditions are fulfilled, as well as the expected narrowing of the central fringe associated with the levitating wave packets. Falling wave packets yield secondary fringe patterns with shifted resonant frequencies, which induce an asymmetry in the central fringe if the total lower state population is monitored. This effect, critical for a clock operation, can nonetheless be efficiently attenuated by limiting the detection zone to the vicinity of the levitating arches. This strategy improves as the levitation time increases: the main contribution to the “falling” background comes then from atoms with a greater downward momentum and thus

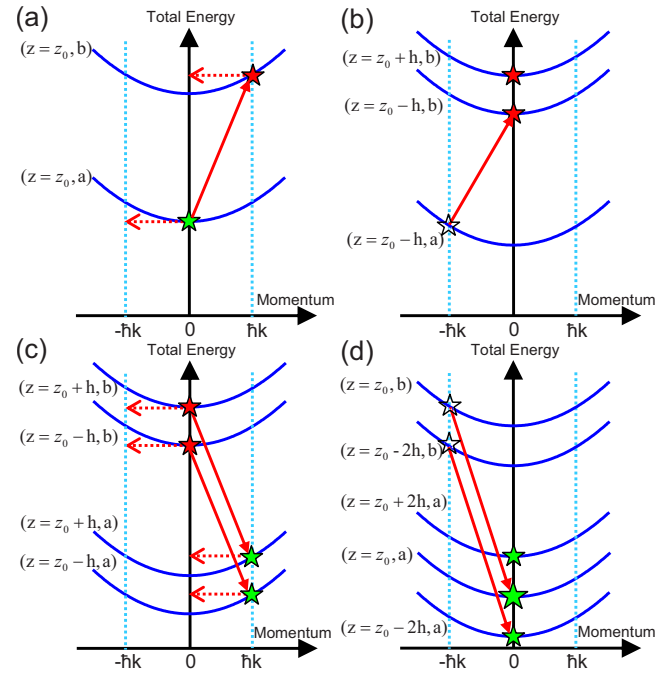


FIG. 4. (Color online) Motion of the atomic wave packets in the energy-momentum picture for the interferometer duration $2T^0$. (a), (b), (c), and (d) associated with the first, second, third, and fourth light pulses, respectively, show the packets present in coherent superposition (full stars) immediately after—or transferred (transparent stars) during—the considered pulse, whose effect is represented by a full red arrow.

further away from the detection zone. Besides, multiple-wave interferences sharpen the symmetric “levitating” central fringe fast enough to limit the effect of the asymmetric background of falling fringes. Considering a shift δT from the resonant duration T_0 , one obtains also a central fringe narrowing as the number of pulses increases and thus an improved determination of acceleration g through condition (3) [10,11]. Multiple-wave interferences thus improve the setup sensitivity in both the inertial and the frequency domains.

To keep the sample within the laser beam diameter, it is necessary to use a transverse confinement, which may be obtained by using laser waves of spherical wave front for the pulses [11]. In contrast to former horizontal clocks [4], the atomic motion is here collinear to the light beam, which reduces the frequency shift resulting from the wave-front curvature. A weak-field treatment, to be published elsewhere, shows that this shift is proportional to the ratio $\Delta\omega_{\text{curv}} \propto k\langle v_{\perp}^2 \rangle T/R$, involving the average square transverse velocity $\langle v_{\perp}^2 \rangle$ and the field radius of curvature R at the average altitude of the levitating cloud. Let us note that our proposal implies technological issues which must be solved to achieve accurate measurements, but they are no more challenging than those of current atomic clocks and sensors. The final population in a given internal state can be monitored by using a time-of-flight absorption imaging with a resonant horizontal laser probe [10].

An analysis of the atomic motion in momentum space, sketched in the energy-momentum diagram of Fig. 4, is es-

pecially enlightening. In this picture, the total energy accounts for the rest mass and the kinetic and the gravitational potential energies. It is a parabolic function of the momentum. Each star stands for a specific wave packet, the motion of which between the light pulses is represented by horizontal dashed arrows, in accordance with energy conservation. For the duration $T:=T^0$, and for a sufficiently coherent atomic sample, Fig. 4 reveals that the atomic motion in momentum is periodic and bounded between two well-defined values associated with the photon recoil. The momentum confinement is provided here by destructive interferences which shut off the quantum channels going out of this bounded momentum region. This remarkable property suggests an analogy with an atomic resonator in momentum space. Following this picture, we have computed the lower-state wave function after N resonant pulse sequences of duration $2T_0$, considering only the vertical axis with no loss of generality. Each wave packet ends up at rest, and with a momentum dispersion Δp_f . Applying the phase relation (1) successively between the multiple arms, one obtains $\psi_a(p, t_0 + 2NT_0) = C_N e^{-p^2/\Delta p_f^2} \sum_{\text{Paths}} e^{-iz_f p}$. C_N is a complex number and the altitudes z_f are the end points of the resonant paths drawn on Fig. 2, on which the sum is performed. By labeling these paths with the instants of momentum transfer, this sum appears up to a global phase as an effective canonical partition function of N independent particles, with $Z_1 = 2 \cos^2(kTp/2m)$ as the one-particle partition function. This yields a wave function of the form $\psi_a(p, t_0 + 2NT_0) = C'_N e^{i\phi(p, N)} e^{-p^2/\Delta p_f^2} \cos^{2N}(p/p_m)$, with $p_m = 2m/kT_0$. As $N \rightarrow +\infty$, multiple-wave interferences thus yield an exponential momentum localization, scaled by the momentum p_m , around the rest value $p=0$. The diffusion in altitude observed in the network of paths of Fig. 2 reflects a back action of this localization.

To summarize, we have proposed a space-time atomic sensor achieving the levitation of an atomic sample through multiple-wave interference effects in a series of vertical $\pi/2$ light pulses. The sensitivity of this levitation toward a double resonance condition can be used to realize a frequency or an acceleration measurement, with a sensitivity improving with the number of interfering wave packets. The sample needs to be cooled at a nanokelvin temperature in order to yield the desired interference effects. At resonance, constructive multiple-wave interferences then maintain the full atomic population in suspension in spite the great number of non-levitating paths. For a sufficiently diluted cloud, transverse confinement may be provided by the wave front of spherical light pulses. In this system, light shifts are due only to a resonant light field and thus expected to be small. This proposal opens promising perspectives for the development of cold atom gravimeters [17] and optical clocks [4–7]. It may also be turned into an atomic gyrometer [2, 19] by using additional horizontal light pulses and exploiting the transverse wave-packet motion.

Note added in proof. The system may also work with ultracold fermionic clouds. As the recent experiment of [20], our system implements a quantum random walk [21], but here it involves a macroscopic number of atoms propagating in free space.

The authors thank S. Bize, P. Bouyer, A. Clairon, A. Landragin, Y. LeCoq, P. Lemonde, F. Pereira, and P. Wolf for stimulating discussions and A. Landragin and S. Walborn for manuscript reading and suggestions. F.I. thanks N. Zagury and L. Davidovich for hospitality. This work was supported by CNRS, DGA (Contract No. 0860003), and Ecole Polytechnique.

-
- [1] C. J. Bordé *et al.*, Phys. Rev. A **30**, 1836 (1984).
 [2] C. J. Bordé, Phys. Lett. A **140**, 10 (1989).
 [3] *Atom Interferometry*, edited by P. R. Berman (Academic Press, New York, 1997).
 [4] G. Wilpers *et al.*, Metrologia **44**, 146 (2007).
 [5] T. Trebst *et al.*, IEEE Trans. Instrum. Meas. **50**, 535 (2001).
 [6] A. D. Ludlow *et al.*, Science **319**, 1805 (2008); R. LeTargat *et al.*, Phys. Rev. Lett. **97**, 130801 (2006); M. Takamoto *et al.*, J. Phys. Soc. Jpn. **75**, 104302 (2006).
 [7] H. Katori, M. Takamoto, V. G. Palchikov, and V. D. Ovsianikov, Phys. Rev. Lett. **91**, 173005 (2003).
 [8] S. Blatt *et al.*, Phys. Rev. Lett. **100**, 140801 (2008); T. Rosenband *et al.*, Science **319**, 1808 (2008).
 [9] M. Weitz, T. Heupel, and T. W. Hänsch, Phys. Rev. Lett. **77**, 2356 (1996); H. Hinderthür, Phys. Rev. A **59**, 2216 (1999); T. Aoki, M. Yasuhara, and A. Morinaga, *ibid.* **67**, 053602 (2003).
 [10] K. J. Hughes, J. H. T. Burke, and C. A. Sackett, Phys. Rev. Lett. **102**, 150403 (2009).
 [11] F. Impens, P. Bouyer, and C. J. Bordé, Appl. Phys. B: Lasers Opt. **84**, 603 (2006).
 [12] C. J. Bordé, in *Frequency Standards and Metrology*, edited by A. De Marchi (Springer, Berlin, 1989), p. 196; M. Ben Dahan, E. Peik, J. Reichel, Y. Castin, and C. Salomon, Phys. Rev. Lett. **76**, 4508 (1996); R. Battesti *et al.*, *ibid.* **92**, 253001 (2004); M. Fattori *et al.*, *ibid.* **100**, 080405 (2008).
 [13] This assumption does not induce any loss of generality: the following discussion would also apply to any mode of the Hermite-Gauss basis, and thus to any wave function by linearity.
 [14] This equation can also be interpreted as a generalized optical path in five dimensions. This formalism is presented in C. J. Bordé, *Proceedings of the Enrico Fermi International School of Physics, 2007* (Academic, New York, 2007), Vol. 168; Eur. Phys. J. Spec. Top. **163**, 315 (2008).
 [15] In the configuration of Fig. 2, the two pulse pairs are performed successively, which maximizes the interferometric area for a fixed interferometer duration; one could nonetheless also let a finite time between them.
 [16] C. J. Bordé, Metrologia **39**, 435 (2002).
 [17] A. Peters, K. Y. Chung, and S. Chu, Nature (London) **400**, 849 (1999); Metrologia **38**, 25 (2001).
 [18] F. Impens and C. J. Bordé, Phys. Rev. A **79**, 043613 (2009); F. Impens, e-print arXiv:0904.0150.
 [19] See B. Canuel *et al.*, Phys. Rev. Lett. **97**, 010402 (2006), and references therein.
 [20] Michal Karski *et al.*, Science **325**, 5937 (2009).
 [21] Y. Aharonov, L. Davidovich, and N. Zagury, Phys. Rev. A **48**, 1687 (1993).